On the formation of highly oxidized pollutants by autoxidation of terpenes under low-temperature-combustion conditions: the case of limonene and α -pinene

Roland Benoit, Nesrine Belhadj, Zahraa Dbouk, Maxence Lailliau, Philippe Dagaut

On the formation of highly oxidized pollutants by autoxidation of terpenes under low-temperature-combustion conditions: the case of limonene and α-pinene

Roland Benoit[1], **Nesrine Belhadj**[1,2], **Zahraa Dbouk**[1,2], **Maxence Lailliau**[1,2], **and Philippe Dagaut**[1]

[1]CNRS-INSIS, ICARE, Orléans, France
[2]Université d'Orléans, Orléans, France

Correspondence: Roland Benoit (roland.benoit@cnrs-orleans.fr)

Received: 8 September 2022 – Discussion started: 11 October 2022
Revised: 14 April 2023 – Accepted: 21 April 2023 – Published: 23 May 2023

Abstract. The oxidation of monoterpenes under atmospheric conditions has been the subject of numerous studies. They were motivated by the formation of oxidized organic molecules (OOMs), which, due to their low vapor pressure, contribute to the formation of secondary organic aerosols (SOA). Among the different reaction mechanisms proposed for the formation of these oxidized chemical compounds, it appears that the autoxidation mechanism, involving successive events of O_2 addition and H migration, common to both low-temperature-combustion and atmospheric conditions, leads to the formation of highly oxidized products (HOPs). However, cool-flame oxidation ($\sim$ 500–800 K) of terpenes has not received much attention even if it can contribute to atmospheric pollution through biomass burning and wildfires. Under such conditions, terpenes can be oxidized via autoxidation. In the present work, we performed oxidation experiments with limonene–oxygen–nitrogen and α-pinene–oxygen–nitrogen mixtures in a jet-stirred reactor (JSR) at 590 K, a residence time of 2 s, and atmospheric pressure. Oxidation products were analyzed by liquid chromatography, flow injection, and soft-ionization–high resolution mass spectrometry. H–D exchange and 2,4-dinitrophenyl hydrazine derivatization were used to assess the presence of OOH and C=O groups in oxidation products, respectively. We probed the effects of the type of ionization used in mass spectrometry analyses on the detection of oxidation products. Heated electrospray ionization (HESI) and atmospheric-pressure chemical ionization (APCI) in positive and negative modes were used. We built an experimental database consisting of literature data for atmospheric oxidation and presently obtained combustion data for the oxidation of the two selected terpenes. This work showed a surprisingly similar set of oxidation products' chemical formulas, including oligomers, formed under the two rather different conditions, i.e., cool-flame and simulated atmospheric oxidation. Data analysis (in HESI mode) indicated that a subset of chemical formulas is common to all experiments, independently of experimental conditions. Finally, this study indicates that more than 45 % of the detected chemical formulas in this full dataset can be ascribed to an autoxidation reaction.

1 Introduction

Terpenes are emitted into the troposphere by vegetation (Seinfeld and Pandis, 2006). They can be used as drop-in fuels (Harvey et al., 2010, 2015; Mewalal et al., 2017), which could increase emissions via fuel evaporation and unburnt fuel release. Biomass burning and wildfires can also release terpenes and their products of oxidation into the troposphere (Gilman et al., 2015; Hatch et al., 2019; Schneider et al., 2022). Wildfire temperature ranges from 573 to 1373 K (Wotton et al., 2012), which covers both the cool-flame ($\sim$ 500–800 K) and intermediate- to high-temperature-combustion regimes. Products of biomass burning have been characterized earlier (Smith et al., 2009). Using van Krevelen diagrams, the authors reported H/C versus O/C in the ranges 0.5 to 3 and 0 to 1, respectively. Whereas a large fraction of these products can derive from cellulose, hemicellulose, and lignin oxidation, their formation via terpene oxidation cannot be ruled out. In a more recent study (Gilman et al., 2015), it was reported that biomass burning emissions were dominated by oxidized organic compounds (57 % to 68 % of total mass emissions). Wildfires are becoming more and more frequent, and their intensity is increasing (Burke et al., 2021). In large wildfires, there are many updrafts, which can transport a variety of materials ranging from gases to particulates and even bacteria (Kobziar et al., 2018). Furthermore, it was recently demonstrated that recent wildfires in Australia produced smoke which could reach an altitude of 35 km (Khaykin et al., 2020). Such events could contribute to ozone destruction (Bernath et al., 2022) but also to tropospheric pollution. However, field measurements are not appropriate for comparison with the present data because a strict distinction of the origins of the chemical compounds observed cannot be assessed. For example, literature works and reviews (Hu et al., 2018; Popovicheva et al., 2019; Prichard et al., 2020) present field measurements from smoldering fires which were not detailed enough to be used here.

Cool-flame oxidation is dominated by autoxidation (Bailey and Norrish, 1952; Benson, 1981; Cox and Cole, 1985; Korcek et al., 1972), which involves peroxy radicals (ROO•). Autoxidation is based on an H shift and oxygen addition, which starts with the initial production of ROO•. This mechanism can repeat itself several times and lead to recurrent oxygen additions to form highly oxidized products (Wang et al., 2017, 2018; Belhadj et al., 2020, 2021a, b):

$$\mathrm{R}\bullet + \mathrm{CO_2} \rightleftarrows \mathrm{ROO}\bullet \text{ (first } \mathrm{O_2}\text{addition)} \quad \text{(R1)}$$

$$\mathrm{ROO}\bullet \rightleftarrows \mathrm{QOOH} \text{ (Hshift)} \quad \text{(R2)}$$

$$\bullet\mathrm{QOOH} + \mathrm{O_2} \rightleftarrows \bullet\mathrm{OOQOOH} \text{ (second } \mathrm{O_2}\text{addition)} \quad \text{(R3)}$$

$$\bullet\mathrm{OOQOOH} \rightleftarrows \mathrm{HOOQ}\bullet'\mathrm{OOH} \text{ (Hshift)} \quad \text{(R4)}$$

$$\mathrm{HOOQ}\bullet'\mathrm{OOH} + \mathrm{O_2} \rightleftarrows (\mathrm{HOO})_2\mathrm{Q}'\mathrm{OO}\bullet \text{ (third } \mathrm{O_2}\text{addition)} \quad \text{(R5)}$$

$$(\mathrm{HOO})_2\mathrm{Q}'\mathrm{OO}\bullet \rightleftarrows (\mathrm{HOO})_2\mathrm{Q}\bullet''\mathrm{OOH} \text{ (Hshift)} \quad \text{(R6)}$$

$$(\mathrm{HOO})_2\mathrm{Q}\bullet''\mathrm{OOH} + \mathrm{O_2} \rightleftarrows (\mathrm{HOO})_3\mathrm{Q}''\mathrm{OO}\bullet \text{ (fourth Oaddition), etc.} \quad \text{(R7)}$$

There, the formation of highly oxidized products (HOPs) was mainly attributed to autoxidation reactions (Belhadj et al., 2021c; Benoit et al., 2021).

In atmospheric chemistry, it is only relatively recent that this pathway has been considered (Vereecken et al., 2007; Crounse et al., 2013; Jokinen et al., 2014a, 2015; Ehn et al., 2014; Berndt et al., 2015, 2016; Iyer et al., 2021). Also, it has been identified that highly oxygenated organic molecules (HOMs), a source of secondary organic aerosols (SOAs), can result from autoxidation processes (Ehn et al., 2014; Wang et al., 2021; Tomaz et al., 2021; Bianchi et al., 2019). Modeling studies complemented by laboratory experiments showed that autoxidation mechanisms proceed simultaneously on different ROO•, leading to the production of a wide range of oxidized compounds in a few hundredths of a second (Jokinen et al., 2014a; Berndt et al., 2016; Bianchi et al., 2019; Iyer et al., 2021). Recent works have shown that, under certain atmospheric conditions, this autoxidation mechanism could be competitive with other reaction pathways involving ROO• (Bianchi et al., 2019), e.g., the carbonyl channel ($\mathrm{ROO}\bullet \rightarrow \mathrm{R}_{-H}\mathrm{O} + \mathrm{OH}$), the hydroperoxide channel ($\mathrm{ROO}\bullet + \mathrm{HOO}\bullet \rightarrow \mathrm{ROOH} + \mathrm{O_2}$ and $\mathrm{RO}\bullet + \bullet\mathrm{OH} + \mathrm{O_2}$), disproportionation reactions ($\mathrm{ROO}\bullet + \mathrm{R'OO}\bullet \rightarrow \mathrm{RO}\bullet + \mathrm{R'O}\bullet + \mathrm{O_2}$ and $\mathrm{R}_{-H}\mathrm{O} + \mathrm{R'OH} + \mathrm{O_2}$), and accretion reactions ($\mathrm{ROO}\bullet + \mathrm{R'OO}\bullet \rightarrow \mathrm{ROOR'} + \mathrm{O_2}$). Similarity, in terms of observed chemical formulas of products from cool-flame oxidation of limonene and atmospheric oxidation of limonene, has been reported recently (Benoit et al., 2021). The same year, Wang et al. (2021) showed that the oxidation of alkanes follows this autoxidation mechanism under both atmospheric and combustion conditions (Wang et al., 2021). Also, that work confirmed that internal H shifts in autoxidation can be promoted by the presence of functional groups, as predicted earlier (Otkjær et al., 2018) for ROO• containing OOH, OH, $\mathrm{OCH_3}$, $\mathrm{CH_3}$, C = O, or C = C groups. Autoxidation will preferentially form chemical functions such as carbonyls, hydroperoxyl, or peroxyl. This large diversity of chemical functions will promote the formation of isomers. Nevertheless, the common point to these chemical compounds is the sequential addition of $\mathrm{O_2}$. Therefore, in a database, potential candidate products of autoxidation are easily identified by this sequential addition.

To better understand the importance of these reaction pathways, the experimental conditions unique to these two chemistries must be considered. In laboratory studies conducted under simulated atmospheric conditions, oxidation occurs at near-ambient temperatures (250–300 K); at atmospheric pressure; and in the presence of ozone and/or •OH

radicals (Table S1 in the Supplement), used to initiate oxidation with low initial terpene concentrations. In combustion, the •OH radical, temperature, and pressure are driving autoxidation. In addition to the increase in temperature, the initial concentrations of the reagents are generally higher compared to the atmospheric conditions in order to initiate the oxidation with O_2, which is much slower than that involving ozone or •OH. Rising temperature increases isomerization rates and favors autoxidation, at the expense of other possible reactions of ROO•. Indeed, it has been reported earlier that a temperature rise from 250 to 273 K does not affect the distribution of HOMs (Quéléver et al., 2019), whereas Tröstl et al. (2016) suggested that the distribution of HOMs is affected by temperature, α-pinene, or particle concentration (Tröstl et al., 2016). Similarly, the experiments of Huang et al. (2018) performed at different temperatures (223 and 29 K) and precursor concentrations (α-pinene 0.714 and 2.2 ppm) suggested that the physicochemical properties, such as the composition of the oligomers (at the nanometer scale), can be affected by a variation in temperature (Huang et al., 2018). The broad range of chemical molecules formed and the impact of the experimental conditions on their character remain subjects for atmospheric chemistry as well as for combustion chemistry studies. Whatever the mechanism of aerosols formation, i.e., oligomerization, functionalization, or accretion, their composition will be linked to that of the initial radical pool (Camredon et al., 2010; Meusinger et al., 2017; Tomaz et al., 2021).

In low-temperature combustion, when the temperature is increased, fuel's autoxidation rate goes through a maximum between 500 and 670 K, depending on the nature of the fuel (Belhadj et al., 2020, 2021c). In low-temperature-combustion chemistry as in atmospheric chemistry, the oxidation of a chemical compound leads to the formation of several thousand chemical products which result from successive additions of oxygen, isomerization, accretion, fragmentation, and oligomerization (Benoit et al., 2021; Belhadj et al., 2021b). The exhaustive analysis of chemical species remains, under the current instrumental limitations, impossible. Indeed, this would consist of analyzing several thousand molecules using separative techniques such as ultra-high-pressure liquid chromatography (UHPLC) or ion mobility spectrometry (IMS) (Krechmer et al., 2016; Kristensen et al., 2016). Nevertheless, it is possible to classify these molecular species, considering only $C_xH_yO_z$ compounds, according to criteria accessible via graphic tool representation such as van Krevelen diagrams, double-bond equivalent (DBE) number, and average carbon oxidation state (OSc) versus the number of carbon atoms (Kourtchev et al., 2015; Nozière et al., 2015). Such postprocessing of large datasets has the advantage of immediately highlighting classes of compounds or physicochemical properties such as the condensation of molecules (vapor pressure), the large variety of oxidized products ($C_xH_yO_1$ to 15 in the present experiments), and the formation of oligomers (Kroll et al., 2011; Xie et al., 2020).

In addition to the recent studies focusing on the first steps of autoxidation, a more global approach, based on the comparison of possible chemical transformations related to autoxidation in low-temperature-combustion and atmospheric chemistry, is needed for evaluating the importance of autoxidation under tropospheric and low-temperature-combustion conditions. In order to study the effects of experimental conditions on the diversity of chemical molecules formed by autoxidation, we have selected α-pinene and limonene, two isomeric terpenes among the most abundant in the troposphere (Zhang et al., 2018). Limonene has a single-ring structure and two double bonds, one of which is exocyclic. α-Pinene has a bicyclic structure and a single endocyclic double bond. These two isomers with their distinctive physicochemical characters are good candidates for studying autoxidation versus initial chemical structure and temperature. For α-pinene, in addition to the reactivity of its endocyclic double bond, products of ring opening of the cyclobutyl group have been detected (Kurtén et al., 2015; Iyer et al., 2021), which could explain the diversity of observed oxidation products. This large pool of oxidation products is increased in the case of limonene by the presence of two double bonds (Hammes et al., 2019; Jokinen et al., 2015).

The present work extends that concerning the oxidation of limonene alone (Benoit et al., 2021). Compared to previous works, we have added the study of α-pinene oxidation to that of limonene and investigated the impact of ionization modes on the number of molecules detected and their chemical nature (unsaturation, oxidation rate). The size of the experimental and bibliographic databases has been increased by more than 50 %, in particular by adding data specific to autoxidation (Krechmer et al., 2016; Tomaz et al., 2021) and references to α-pinene (Table 2). Here, we oxidized α-pinene and limonene in a jet-stirred reactor at atmospheric pressure, excess of oxygen, and elevated temperature. We characterized the impact of using different ionization techniques (heated electrospray ionization, HESI, and APCI, atmospheric-pressure chemical ionization) in positive and negative modes on the pool of detected chemical formulas. The particularities of each ionization mode were analyzed to identify the most suitable ionization technique for exploring the formation of autoxidation products under low-temperature combustion. H–D exchange and 2,4-dinitrophenyl hydrazine derivatization were used to assess the presence of hydroperoxy and carbonyl groups, respectively. Chemical formulas detected here and in atmospheric-chemistry studies were compiled and tentatively used to evaluate the importance of autoxidation routes under both conditions.

2 Experiments

2.1 Oxidation experiments

The present experiments were carried out in a fused-silica jet-stirred reactor (JSR) setup presented earlier (Dagaut et al., 1986, 1988) and used in previous studies (Dagaut et al., 1987; Benoit et al., 2021; Belhadj et al., 2021c). We studied the oxidation of the two isomers, α-pinene and limonene, separately. As in earlier works (Benoit et al., 2021; Belhadj et al., 2021c), α-pinene (+), 98 % pure from Sigma Aldrich, and limonene (R)-(+), > 97 % pure from Sigma Aldrich, were pumped by an HPLC pump (Shimadzu LC10 AD VP) with an online degasser (Shimadzu DGU-20 A3) and sent to a vaporizer assembly, where they were diluted by a nitrogen flow. Each terpene isomer and oxygen atom, both diluted by N_2, was sent separately to a 42 mL JSR to avoid oxidation before reaching four injectors (nozzles of 1 mm i.d.) providing stirring. The flow rates of nitrogen and oxygen were controlled by mass flow meters. Good thermal homogeneity along the vertical axis of the JSR was recorded (gradients of $< 1\,\mathrm{K\,cm^{-1}}$) by thermocouple measurements (0.1 mm Pt-Pt/Rh-10 % wires located inside a thin-wall silica tube). In order to observe the oxidation of these isomers, which are not prone to strong self-ignition, the oxidation of 1 % of these chemical compounds ($C_{10}H_{16}$) under fuel-lean conditions (equivalence ratio 0.25, 56 % O_2, 43 % N_2) was carried out at 590 K, atmospheric pressure, and a residence time of 2 s. Under these conditions, the oxidation of the two isomers is initiated by slow H-atom abstraction by molecular oxygen ($RH + O_2 \rightarrow R\bullet + HO_2\bullet$). The fuel radicals R• react rapidly with O_2 to form peroxy radicals which undergo further oxidation, characteristic of autoxidation. Nevertheless, this autoxidation mechanism, although predominant, is not exclusive, and other oxidation mechanisms are possible (Belhadj et al., 2021b). In this case, there may be a random overlap of chemical formulas. The autoxidation criteria (two chemical formulas separated by two oxygen atoms) allow these overlaps to be limited or avoided.

2.2 Chemical analyses

A 2 mm i.d. probe was used to collect samples. To measure low-temperature-oxidation products ranging from early oxidation steps to highly oxidized products, the samples were bubbled into cooled acetonitrile (UHPLC grade ≥ 99.9, T = 0 °C, 250 mL) for 90 min. The resulting solution was stored in a freezer at −15 °C. The stability of the products was verified. No detectable changes in the mass spectra were observed after more than 1 month, which is consistent with previous findings (Belhadj et al., 2021c).

Analyses of samples collected in acetonitrile (ACN) were carried out via direct infusion (rate: $3\,\mu\mathrm{L\,min^{-1}}$; recorded for 1 min for data averaging) in the ionization chamber of a high-resolution mass spectrometer (Thermo Scientific Orbitrap® Q Exactive, mass resolution 140 000 and mass accuracy < 0.5 ppm RMS). UHPLC conditions were a Thermo Fisher Scientific Vanquish UHPLC with a C18 column (Phenomenex Luna, 1.6 µm, 110 Å, 100 × 2.1 mm). The column temperature was maintained at 40 °C. A total of 3 µmL of sample was eluted by a mobile phase containing a water–ACN mixture (pure water, ACN HPLC grade) at a flow rate of $250\,\mu\mathrm{L\,min^{-1}}$ (gradient: 5 % to 20 % ACN – 3 min, 20 % to 65 % ACN – 22 min, 65 % to 75 % ACN – 4 min, 75 % to 90 % ACN – 4 min, for a total of 33 min).

Both HESI and APCI were used in positive and negative modes for the ionization of products. The HESI settings were spray voltage of 3.8 kV, vaporizer temperature of 150 °C, capillary temperature of 200 °C, sheath gas flow of 8 arbitrary units (a.u.), auxiliary gas flow of 1 a.u., and sweep gas flow of 0 a.u. In APCI, the settings were corona discharge current of 3 µA, spray voltage of 3.8 kV, vaporizer temperature of 150 °C, capillary temperature of 200 °C, sheath gas flow of 8 a.u., auxiliary gas flow of 1 a.u., and sweep gas flow of 0 a.u. In order to avoid transmission and detection effects of ions depending on their mass inside the C trap (Hecht et al., 2019), acquisitions with three mass ranges were performed (m/z 50–750, m/z 150–750, m/z 300–750). The upper limit of m/z 750 was chosen because of the absence of a signal beyond this value. It was shown that no significant oxidation occurred in the HESI and APCI ion sources by injecting a limonene–ACN mixture (Fig. S1 in the Supplement). The optimization of the Orbitrap ionization parameters in HESI and APCI did not show any clustering phenomenon for these two monoterpene isomers. The parameters evaluated were injection source, capillary distance, vaporization and capillary temperatures, applied difference in potential, injected volume, and flow rate of nitrogen in the ionization source. Positive and negative HESI mass calibrations were performed using Pierce™ calibration mixtures (Thermo Scientific). Chemical compounds with relative intensity less than 1 ppm to the highest MS signal in the mass spectrum were not considered. Nevertheless, it should be considered that some of the molecules presented in this study could result from our experimental conditions (continuous-flow reactor, reagent concentration, temperature, reaction time) and to some extent from our acquisition conditions, different from those in the previous studies (Deng et al., 2021; Quéléver et al., 2019; Meusinger et al., 2017; Krechmer et al., 2016; Tomaz et al., 2021; Fang et al., 2017; Witkowski and Gierczak, 2017; Jokinen et al., 2015; Nørgaard et al., 2013; Bateman et al., 2009; Walser et al., 2008; Warscheid and Hoffmann, 2001; Hammes et al., 2019; Kundu et al., 2012). Operating with a continuous-flow reactor at elevated temperature and high initial concentration of reagents allows the formation of combustion-relevant products, which does not exclude their possible formation under atmospheric conditions. To assess the formation of products containing OOH and C=O groups, as in previous works (Belhadj et al., 2021a, b),

Table 1. Number of ions detected for each source in positive and negative modes (by protonation or deprotonation, respectively).

Ionization source	α-pinene		Limonene	
APCI	646 $(R+H)^+$	503 $(R-H)^-$	1321 $(R+H)^+$	1346 $(R-H)^-$
HESI	594 $(R+H)^+$	693 $(R-H)^-$	1017 $(R+H)^+$	1864 $(R-H)^-$

H–D exchange with D_2O and 2,4-dinitrophenyl hydrazine derivation were used, respectively.

3 Data processing

High-resolution mass spectrometry (HR-MS) generates large datasets, which are difficult to fully analyze by sequential methods. When the study requires the processing of several thousand molecules, the use of statistical tools and graphical representation means becomes necessary. In this study, we have chosen to use the van Krevelen diagram (Van Krevelen, 1950) by adding an additional dimension, the double-bond equivalent (DBE). The DBE number represents the sum of unsaturation and rings present in a chemical compound (Melendez-Perez et al., 2016). The interest of this type of representation is to be able to identify more easily the clusters (increase in the DBE number at constant O/C and H/C ratios):

$$\mathrm{DBE} = 1 + \mathrm{C} - \mathrm{H}/2. \tag{R8}$$

This number is independent of the number of O atoms but changes with the number of hydrogen atoms. Decimal values of this number, which correspond to an odd number of hydrogen atoms, were not considered in this study. Then, the superpositions of points (and therefore of chemical formulas) in the O/C versus H/C space are suppressed. The oxidation state of carbon (OSc) provides a measure of the degree of oxidation of chemical compounds (Kroll et al., 2011). This provides a framework for describing the chemistry of organic species. It is defined by the following equation:

$$\mathrm{OSc} \approx 2\mathrm{O}/\mathrm{C} - \mathrm{H}/\mathrm{C}. \tag{R9}$$

4 Results and discussion

We studied the oxidation of α-pinene and limonene ($C_{10}H_{16}$) at 590 K under atmospheric pressure with a residence time of 2 s and a fuel concentration of 1 %. Under these conditions, the formation of peroxides by autoxidation at low temperature should be efficient (Belhadj et al., 2021c), even though the conversion of the fuels remains moderate.

4.1 Characterization of ionization sources

First, we have studied the impact of APCI and HESI sources, in positive and negative modes, on the chemical formulas detected. The HESI and APCI sources in positive and negative mode were used, and their operating parameters were varied, i.e., temperature, gas flow, and accelerating voltage (see Sect. 2). For each polarity, only ions composed of carbon, hydrogen (even numbers), and oxygen were considered. Molecular duplicates inherent to mass range overlaps were excluded. By following these rules, we obtained a different number of ions depending on the ionization source and the polarity used. Table 1 shows the number of ions according to the experimental conditions and the discrimination rules.

Each combination of ionization sources and polarity generated a set of chemical formulas. To make a meaningful comparison between the positive- and negative-ion data, the chemical formulas used were the precursors of the ions identified in the mass spectra. These sets have common data, but also specific chemical formulas. For a given ionization source, ~ 50 % of the chemical formulas are observed whatever the ionization polarity; i.e., using both polarities one can capture between 30 %–50 % more molecular species (since some of them are ionized under a single mode, + or −, depending on their chemical structure). Utilizing both ionization polarities is helpful for identifying a larger quantity of species. The HESI source data were compared to the APCI data (Tables S1 and S2), showing an increased number (20 % to 30 %) of chemical formulas detected by HESI. This increase is characterized by a better detection of negatively ionized species and those with a higher DBE. In order to evaluate further the interest for using these ionization sources, we compiled these data in Venn diagrams and proposed a visualization of these sets with a van Krevelen representation; we added the number of DBE in the third dimension (Tables S1 and S2).

In positive-ionization mode, independently of the ionization source and in addition to the common molecular formulas, we detected products with an O/C ratio < 0.2, whereas in the negative-ionization mode, we detected molecular formulas with an O/C ratio > 0.5. In addition to these observations, we noted that HESI is more appropriate for studying products with a large number of unsaturation (DBE >5), which is probably related to the increase in the number of hydroperoxide and carboxyl groups along with the fact that a heated ionization source favors vaporization of low-volatility compounds. Finally, for an optimal detection of the oxidation products, it is necessary to consider the transmission limits of the C trap. Here, we could increase the number of molecular formulas detected using several mass ranges for

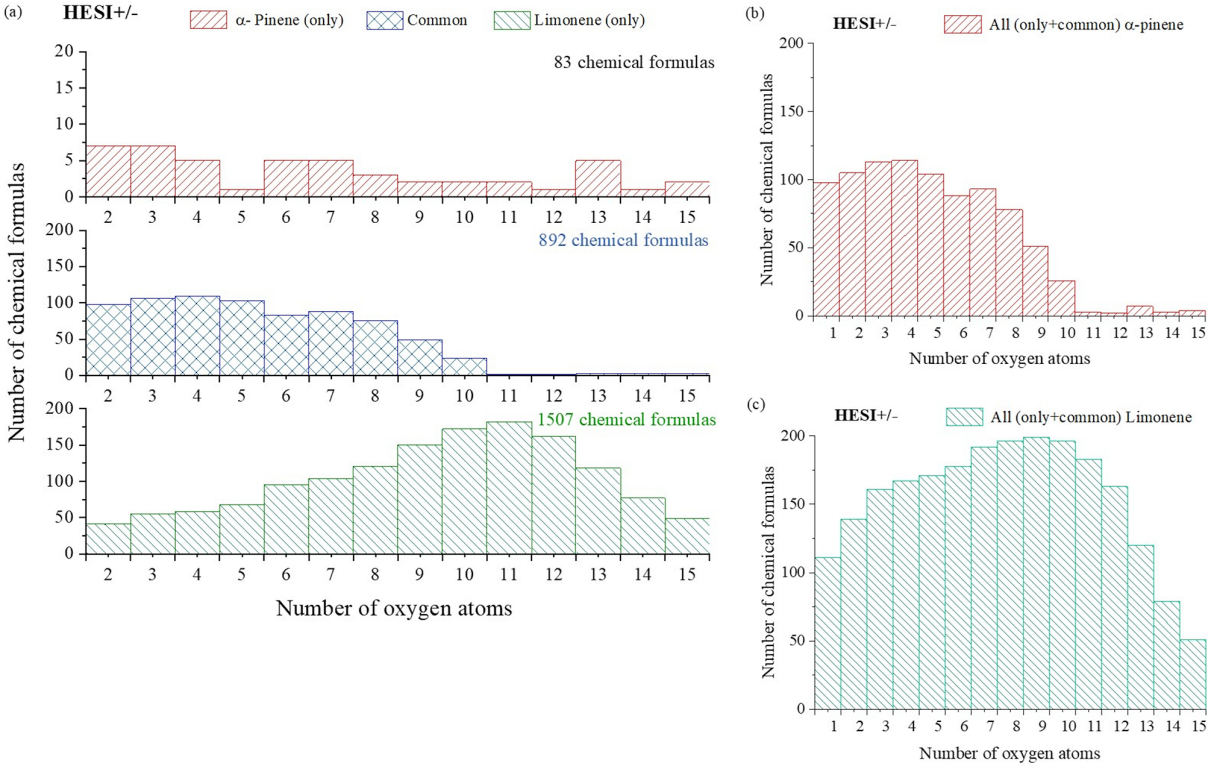

Figure 1. Distribution of α-pinene and limonene oxidation products as a function of their oxygen content (ionization source: HESI, combined positive- and negative-mode data). **(a)** α-Pinene and limonene HESI ($\pm$), **(b)** α-pinene HESI ($\pm$), **(c)** limonene HESI ($\pm$).

data acquisition (Sect. 2.2) by more than 60 %. The most appropriate ionization polarity to be used is tied to chemical functions present in products to be detected. We could increase the number of chemical formulas detected by using both positive- and negative-ionization modes by 30 % to 100 %. Using HESI is consistent with previous findings indicating that ESI is well suited for the ionization of acidic, polar, and heteroatom-containing chemicals (Kekäläinen et al., 2013). To illustrate the present results, HESI(−)–MS spectra are provided in the Supplement (Fig. S2). The list of all chemical formulas found in limonene and α-pinene samples (HESI negative and positive mode) is given in the Supplement.

4.2 Autoxidation products detected in a JSR

In order to compare the oxidation of α-pinene and limonene, we compiled the positive- and negative-ionization data obtained with APCI (Table S1) and HESI (Table S2) ionization sources to obtain a more exhaustive database. For the APCI and HESI sources, we distinguished three datasets, two of which are specific to the oxidation of α-pinene and limonene and one which is common to both isomers. In the following text, "only" is used to describe the molecules specific to the oxidation of one of the isomeric terpenes. This common dataset represents more than 90 % of the chemical formulas identified in the α-pinene oxidation samples detected with APCI or HESI. For limonene, for which the number of identified chemical formulas is larger, regardless of the ionization source, this common dataset represents nearly 40 % of the chemical formulas detected. In these two cases, the relatively low residence time (2 s) and the diversity of the chemical formulas obtained suggest that the oxidation of these two terpene isomers leads to ring opening, a phenomenon also observed in atmospheric chemistry (Berndt et al., 2016; Zhao et al., 2018; Iyer et al., 2021). Concerning the molecular formulas of products common to both isomers, Fig. 1 shows that they are limited to compounds with 10 oxygen atoms or fewer. This limit is linked to α-pinene, whose oxidation beyond 10 oxygen atoms remains weak (fewer than 2 % of the detected molecules for this terpene). In the case of limonene, the presence of an exocyclic double bond will increase, in a similar way to atmospheric chemistry (Kundu et al., 2012), the possibilities of oxidation and accretion. However, it remains impossible, considering the size of the whole dataset and the diversity of the isomers, to formalize all the reaction mechanisms. Nevertheless, the formation of oxidized species can be described with the help of graphical tools. The number of oxygen atoms per molecule indicates that limonene oxidizes more than α-pinene (Fig. 1a). In the case of limonene, with a HESI source, chemicals with an oxygen number of up to 15 were detected. Most of the chemi-

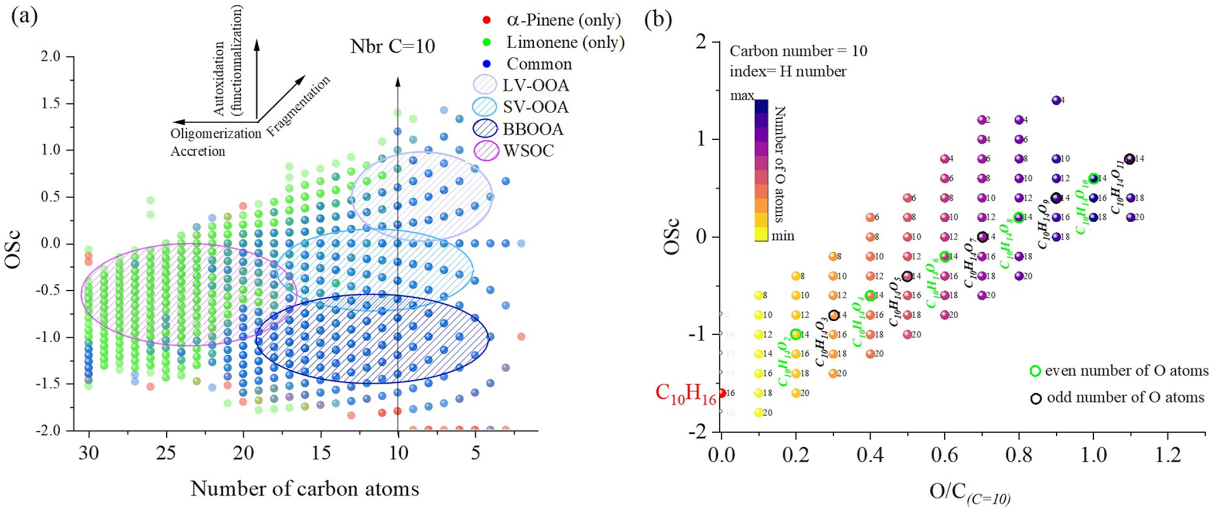

Figure 2. Overview of the distribution of limonene and α-pinene oxidation products observed in a JSR: **(a)** OSc versus carbon number in detected chemical formulas from APCI and HESI data. **(b)** Molecular formulas detected in this study presented in the OSc versus O/C space for a carbon number of 10; index of the products: number of hydrogen atoms.

cal formulas recorded had 8–10 O atoms (Fig. 1c), whereas for α-pinene the products with $>$ 8 O atoms were much less abundant (Fig. 1b). Moreover, for the products specific to limonene oxidation, this graph shows a distribution centered on nine oxygen atoms with carbon skeletons probably resulting from accretion.

To verify this accretion hypothesis, we can plot the OSc as a function of the number of carbon atoms or the O/C ratio at a fixed number of C atoms (Fig. 2). Indeed, the presence of chemical compounds with 11 carbon atoms can be explained by an accretion phenomenon (Wang et al., 2021), but the advantage of this OSc versus nbrC (number of C atoms) space representation (Kroll et al., 2011) is to allow this phenomenon to be studied for all the data. One can visualize the evolution of the molecular oxidation for each carbon skeleton and the formation of oligomers. Species that are unique to one of the isomers or common to both are differentiated using different colors. In addition, in Fig. 2a, we observe mechanisms of fragmentation ($C_{<10}$), accretion, and oligomerization ($C_{>10}$). These reaction mechanisms contribute to forming chemical classes according to their number of carbon atoms, up to C=30. This limit is probably due to the ionization or detection capacity of the spectrometer. The increase in the number of oxygen atoms, but also of carbon atoms, will decrease products' volatility. Following a classification proposed in the literature (Kroll et al., 2011), we distinguished four sets of products: low-volatility oxidized organic aerosols (LV-OOAs), semi-volatile oxidized organic aerosols (SV-OOAs), biomass burning organic aerosols (BBOAs), and water-soluble organic carbons (WSOCs). In the OSc versus carbon number plot (Fig. 2a), the vertical lines (at constant carbon number) are a first criterion for finding potential candidate products of autoxidation. Figure 2b shows, for a fixed number of carbon and hydrogen atoms, the diversity of oxidized species formed. Different oxygen parities are observed, showing that different reaction mechanisms occur.

This parity distinction is initially present for the two main radicals, ROO• and RO•, involved in autoxidation mechanisms. However, termination and propagation reactions will change the oxygen parity (Fig. 3). Then, parity links between radicals and molecules are lost, which prevents interpretation of radical oxidation routes. HESI data showed an equivalent distribution of oxygen parities in molecular products (odd: 51 %; even: 49 %) which cannot allow conclusions on the relative importance of reaction pathways. It should be noted that other reaction mechanisms can also change oxygen parity, e.g., QOOH $\rightarrow$ cyclic ether (QO) + OH (Wang et al., 2017). Figure 2b illustrates the autoxidation products presented in Fig. S3. There, one can see the formation routes to even-oxygen compounds $C_{10}H_{14}O_2$ to 10 and to odd-oxygen compounds $C_{10}H_{14}O_3$ to 11. The molecular formulas detected in our experiments are marked in bold in Fig. 2b. The other formulas presented in Fig. 2b should result from other oxidation pathways. Indeed, products with chemical formulas with H $\geq$ 16 cannot derive from the autoxidation pathways described in Fig. S3. Other pathways (Fig. S5) can yield such species, e.g., through the initial addition of OH to terpenes' double bonds followed by O_2 addition and autoxidation of resulting products.

Nevertheless, despite this change in parity, in the case of autoxidation, the free-radical reaction pathway (shown in Figs. S3 and S5 for both oxygen parities) can produce a set of molecular products that mirrors repeated O_2 addition, characteristic of autoxidation (Fig. 2b). Furthermore, we studied the relative intensities of identified chemical formulas for α-pinene and limonene (HESI source). The results pre-

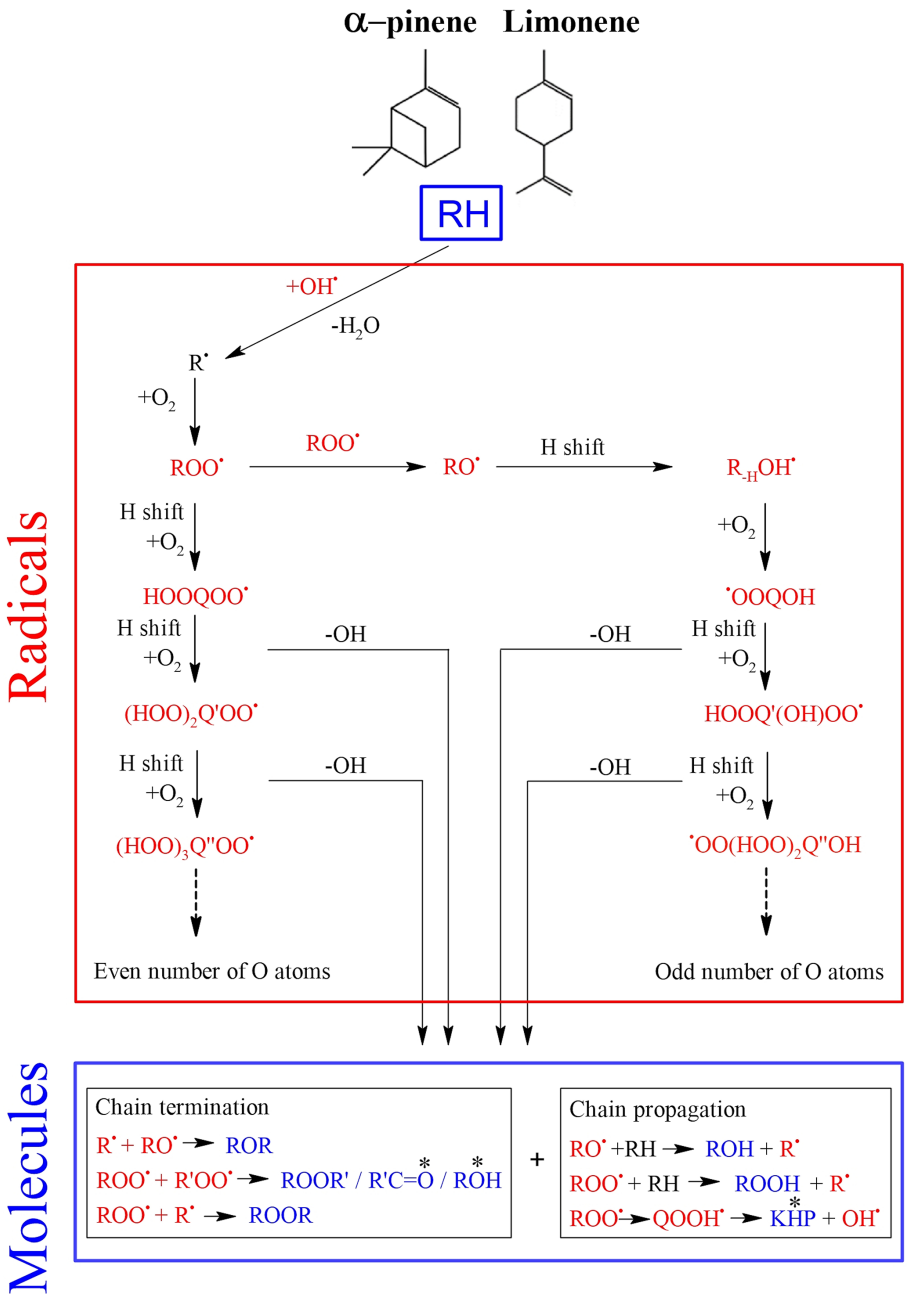

Figure 3. Accepted autoxidation reaction mechanisms in combustion (left) and in the atmosphere (left and right). The change in oxygen atom parity is indicated by "*" (Berndt et al., 2016).

sented in Table 2 show an overall decrease in relative intensities of products' signal with increasing number of oxygen atoms ($C_{10}H_{14}O_{2,4,6,8,...}$, $C_{10}H_{14}O_{3,5,7...}$) for both terpenes. It is clear that the repeated addition of O_2 to radicals (Fig. S3) associated with the decrease in the relative intensities of the products formed is not sufficient to assess an autoxidation mechanism, although it is a necessary step to constrain the identification phase of the isomers, otherwise impossible within sets composed of several thousand chemical molecules. Finally, few chemical formulas with no chemical relevance ($C_xH_4O_y$) were detected. These are probably artifacts linked to the characterization method (ionization mode, ion transfer, ion isolation in the C trap, incorrect mass identification). We chose to leave these data out, knowing that they would be discarded in the various subsequent comparisons.

Table 2. Relative intensities of detected chemical formulas for α-pinene and limonene (HESI− data) which could result from autoxidation of these terpenes. Signal intensities are given in parentheses. Chemical formulas are highlighted in red in the database in the Supplement.

	Limonene	α-pinene
Even number of oxygen atoms		
Hydroxyketone	$C_{10}H_{14}O_2$ ($1.61442 \times 10^{+7}$)	$C_{10}H_{14}O_2$ ($4.54785 \times 10^{+7}$)
$+O_2$ (first)	$C_{10}H_{14}O_4$ ($3.34718 \times 10^{+7}$)	$C_{10}H_{14}O_4$ ($2.52885 \times 10^{+6}$)
$+O_2$ (second)	$C_{10}H_{14}O_6$ ($9.58108 \times 10^{+6}$)	$C_{10}H_{14}O_6$ ($7.56393 \times 10^{+4}$)
$+O_2$ (third)	$C_{10}H_{14}O_8$ ($9.55306 \times 10^{+5}$)	$C_{10}H_{14}O_8$ ($2.91182 \times 10^{+4}$)
$+O_2$ (fourth)	$C_{10}H_{14}O_{10}$ ($1.00597 \times 10^{+4}$)	$C_{10}H_{14}O_{10}$ (not detected)
	$C_{10}H_{14}O_{12}$ (not detected)	–
Odd number of oxygen atoms		
Hydroperoxy carbonyl	$C_{10}H_{14}O_3$ ($3.23297 \times 10^{+7}$)	$C_{10}H_{14}O_3$ ($9.3999 \times 10^{+6}$)
$+O_2$ (first)	$C_{10}H_{14}O_5$ ($2.27278 \times 10^{+7}$)	$C_{10}H_{14}O_5$ ($1.17044 \times 10^{+5}$)
$+O_2$ (second)	$C_{10}H_{14}O_7$ ($4.04207 \times 10^{+6}$)	$C_{10}H_{14}O_7$ ($7.17307 \times 10^{+4}$)
$+O_2$ (third)	$C_{10}H_{14}O_9$ ($1.92816 \times 10^{+5}$)	$C_{10}H_{14}O_9$ (not detected)
$+O_2$ (fourth)	$C_{10}H_{14}O_{11}$ ($6.34129 \times 10^{+3}$)	–
	$C_{10}H_{14}O_{13}$ (not detected)	–

4.3 Combustion versus atmospheric oxidation

4.3.1 Global analysis

We have explored potential chemical pathways related to autoxidation in the previous section. For this purpose, we have performed experiments under cool-flame conditions (590 K). This autoxidation mechanism is also present in atmospheric chemistry, but it has only recently been found that this mechanism could be one of the main formation pathways for SOA (Savee et al., 2015; Crounse et al., 2013; Jokinen et al., 2014a; Iyer et al., 2021). Studies have described this mechanism in the case of atmospheric chemistry with the identification of radicals and molecular species (Tomaz et al., 2021). However, previous studies on the propagation of this reaction mechanism have mainly focused on the initial steps of autoxidation without screening all identified chemical formulas for potential autoxidation products. It is therefore useful to assess the proportion of possible autoxidation products among the total chemical species formed.

Here, we propose a new approach which consists of assessing a set of molecules mainly resulting from autoxidation against different sets of experimental studies related to atmospheric chemistry. The objective is to evaluate similarity of oxidation products formed under these conditions. For this purpose, we selected a HESI ionization source, better suited for detecting higher-polarity oxidized molecules, as well as higher-molecular-weight products (detection of 96 % of the total chemical formulas observed in autoxidation by APCI and HESI).

Among published atmospheric-chemistry studies of terpene oxidation, we have selected 15 studies presenting enough chemical products of oxidation: 4 for α-pinene and 11 for limonene. The data were acquired using different experimental procedures (methods of oxidation, techniques of characterization). Table 3 summarizes all the experimental parameters related to the selected studies. From that table, one can note that few studies involved chromatographic analyses (Tomaz, 2021; Witkowski and Gierczak, 2017; Warscheid and Hoffmann, 2001). The data are from the articles or files provided in Tables S1 and S2. In these studies, oxidation was performed only by ozonolysis with different experimental conditions that gather the main methods described in the literature: ozonolysis, dark ozonolysis, ozonolysis with OH scavenger, ozonolysis with or without seed particles. We considered that the ionization mode used in mass spectrometry did not modify the nature of the chemical species but only the relative detection of ions, depending on the type of ionization used and the sensitivity of the instruments (Riva et al., 2019). The combination of data obtained using (±) HESI gives a rather complete picture of the autoxidation products.

First, we compared the data from ozonolysis studies of each terpene and identified similarities through Venn diagrams. For studies with two ionization sources, duplicate chemical formulas were removed. We selected the four most representative studies by the number of the chemical formulas detected. Then, we compared the set of chemical formulas identified after ozonolysis to those produced in low-temperature combustion, the objective being (i) to highlight similarities in terms of products generated by the two oxidation modes and (ii) to identify chemicals resulting from autoxidation.

For α-pinene oxidation, in the 4 selected studies 567 chemical formulas were detected with all polarities combined. Only one study (Meusinger et al., 2017) was performed in positive-ionization mode, and none of the studies'

Table 3. Experimental settings of 15 oxidation studies of 2 terpenes under atmospheric conditions and cool flames. LC: liquid chromatography; npcs: number of counts per second; PAM: potential aerosol mass; FEP: fluorinated ethylene propylene; API: atmospheric pressure interface; PTR : proton transfer reaction; CI: chemical ionization; IMS: ion mobility spectrometer.

Reference	Oxidation mode	Sampling	Experimental setup	Concentrations of reactants	Ionization/ source	Instrument	Chemical formulas	LC
α-pinene								
Deng et al. (2021)	Dark ozonolysis, seed particles, OH scavenger	Online	Teflon bag, 0.7 m^3	3.3 ± 0.6 ncps per ppbv α-pinene	ESI	Time-of-flight (ToF-MS)	351	No
Quéléver et al. (2019)	Ozonolysis	Online	Teflon bag, 5 m^3	10 and 50 ppb α-pinene	NO_3^- (CI)	CI-APi-ToF	68	No
Meusinger et al. (2017)	Dark ozonolysis, OH scavenger, no seed particles	Offline	Teflon bag, 4.5 m^3	60 ppb α-pinene	Proton transfer	PTR-MS-ToF	153	No
Krechmer et al. (2016)	Ozonolysis	Offline	PAM oxidation reactor	Field measurement	ESI (–) and NO_3^- (CI)	CI-IMS-ToF	43	No
This work	Cool-flame autoxidation	Offline	Jet-stirred reactor 42 mL	1 % α-pinene, no ozone	APCI (3 kV), HESI (3 kV)	Orbitrap® Q Exactive	820 (APCI), 975 (HESI)	Yes
Limonene								
Krechmer et al. (2016)	Ozonolysis	Offline	PAM oxidation reactor	Not specified	ESI (–) and NO_3^- (CI)	CI-IMS-ToF	63	No
Tomaz et al. (2021)	Ozonolysis	Online	Flow tube reactor (18 L)	45–227 ppb limonene	NO_3^- (CI) –	Orbitrap® Q Exactive	199	Yes
Fang et al. (2017)	OH-initiated photooxidation, dark ozonolysis	Online	Smog chamber	900–1500 ppb limonene	UV, 10 eV	Time-of-flight (ToF)	17	No
Witkowski and Gierczak (2017)	Dark ozonolysis	Offline	Flow reactor	2 ppm limonene	ESI, 4.5 kV	Triple quadrupole	12	Yes
Jokinen et al. (2015)	Ozonolysis	Online	Flow glass tube	$1–10\,000 \times 10^9$ molec. cm^{-3} limonene	NO_3^- (CI)	Time-of-flight (ToF)	11	No
Nørgaard et al. (2013)	Ozone (plasma)	Online	Directly on the support	850 ppb ozone 15–150 ppb limonene	Plasma	Quadrupole time-of-flight (QToF)	29	No
Bateman et al. (2009)	Dark and UV radiations, ozonolysis	Offline	Teflon FEP reaction chamber	1 ppm ozone 1 ppm limonene	Modified ESI (±)	LTQ-Orbitrap Hybrid Mass (ESI)	924	No
Walser et al. (2008)	Dark ozonolysis	Offline	Teflon FEP reaction chamber	1–10 ppm ozone, 10 ppm limonene	ESI (±), 4.5 kV	LTQ-Orbitrap Hybrid Mass (ESI)	465	No
Warscheid and Hoffmann (2001)	Ozonolysis	Online	Smog chamber	300–500 ppb limonene	APCI, 3 kV	Quadrupole ion trap mass	21	Yes
Hammes et al. (2019)	Dark ozonolysis	Online	Flow reactor	15, 40, 150 ppb limonene	^{210}Po α acetate ions	HR-ToF-CIMS	20	No
Kundu et al. (2012)	Dark ozonolysis	Offline	Teflon reaction chamber	250 ppb ozone, 500 ppb limonene	ESI, 3.7 and 4 kV	LTQ FT Ultra, Thermo Scientific (ESI)	1197	No
This work	Cool-flame autoxidation	Offline	Jet-stirred reactor 42 mL	1 % limonene, no ozone	APCI (3 µA), HESI (3 kV)	Orbitrap® Q Exactive	1863 (APCI), 2399 (HESI)	Yes

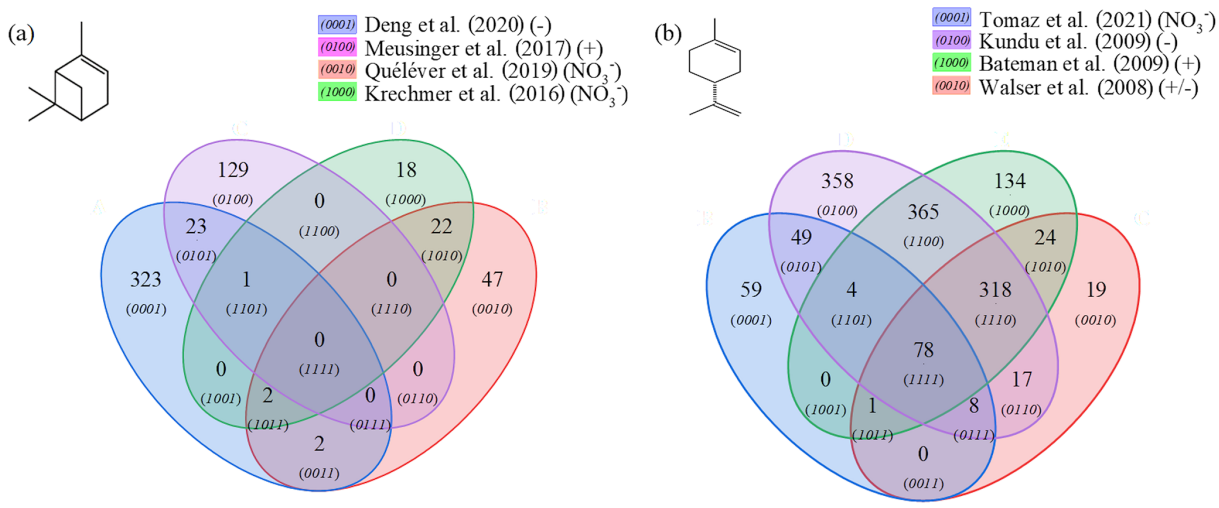

Figure 4. Venn diagrams for comparing the oxidation results from ozonolysis of **(a)** α-pinene and **(b)** limonene (see conditions in Table 1). Each digit indicates a study, and the value of the digit characterizes the presence (value 1) or absence (0) of common products detected in different studies; e.g., 23 chemical formulas (0101) are common to the studies of Deng et al. (2021) (0001) and Meusinger et al. (2017) (0100) **(a)**.

reported data were obtained with two ionization modes ($\pm$). For the oxidation of limonene, the four selected studies identified 1434 chemical formulas. Among these studies, the experiments by Walser et al. (2008) were performed with both positive- and negative-ionization modes. In contrast to the α-pinene case, the selected studies for limonene were performed with similar ionization sources, which probably contributed to increased data similarity (Walser et al., 2008). In the case of limonene oxidation, for which accretion is more important than for α-pinene and for which a greater number of chemical formulas were identified, the similarities are more important (Jokinen et al., 2014b). These results are presented in Fig. 4, where the ionization polarity used in each study is specified.

For α-pinene, no chemical formula is common to all datasets. Different hypotheses can be offered to explain this result. Among them, the number of chemical formulas identified per study remains limited (a few dozen to several hundred), and these small datasets are sometimes restricted to specific mass ranges, e.g., C_{10} to C_{20} (Quéléver et al., 2019). In the case of studies carried out with an NO_3^- source, sensitive to HOMs and produced preferentially by autoxidation, we note that nearly 50 % of the chemical formulas (10/22, 1010) are linked by a simple difference of two oxygen atoms.

For limonene, chemical formulas are common to the four studies selected here. In this dataset, a large majority of chemical formulas show a similar relationship to autoxidation, i.e., a simple difference of two oxygen atoms: 62 % (Tomaz et al., 2021), 54 % (Walser et al., 2008), 69 % (Kundu et al., 2012), 66 % (Bateman et al., 2009), and 72 % (this study). This result seems to indicate that autoxidation dominates.

One can then ask if reaction mechanisms common to atmospheric and combustion chemistry can generate, despite radically different experimental conditions, a set of common chemical formulas and if in this common dataset a common link, characteristic of autoxidation, is observable. To address that question, we compared all the previous results for each of these terpenes to those obtained under the present combustion study. The comparisons were made using our HESI data. One should remember that the oxidation conditions in the JSR were chosen in order to maximize low-temperature autoxidation. Again, we used Venn diagrams to analyze these datasets consisting of 1590 chemical formulas in the case of α-pinene and 5184 chemical formulas in the case of limonene. The results of these analyses are presented in Fig. 5.

It turned out that for α-pinene 301 chemical formulas and for limonene 871 chemical formulas were common to oxidation by ozonolysis (with or without scavenger) and combustion. This represents 31 % of the chemical formulas for the ozonolysis of α-pinene and 36 % for those of limonene ozonolysis. For α-pinene, the similarities compared to combustion are specific to each study: 69 % (243) in Deng et al. (2021), 46 % (71) in Meusinger et al. (2017), 7 % (5) in Quéléver et al. (2019), 23 % (10) in Krechmer et al. (2016). Chemical formulas common to all studies were not identified. This lack of similarity may be due to a partial characterization of the chemical formulas or a weaker oxidation of α-pinene with an ionization mode less favorable to low-molecular-weight products.

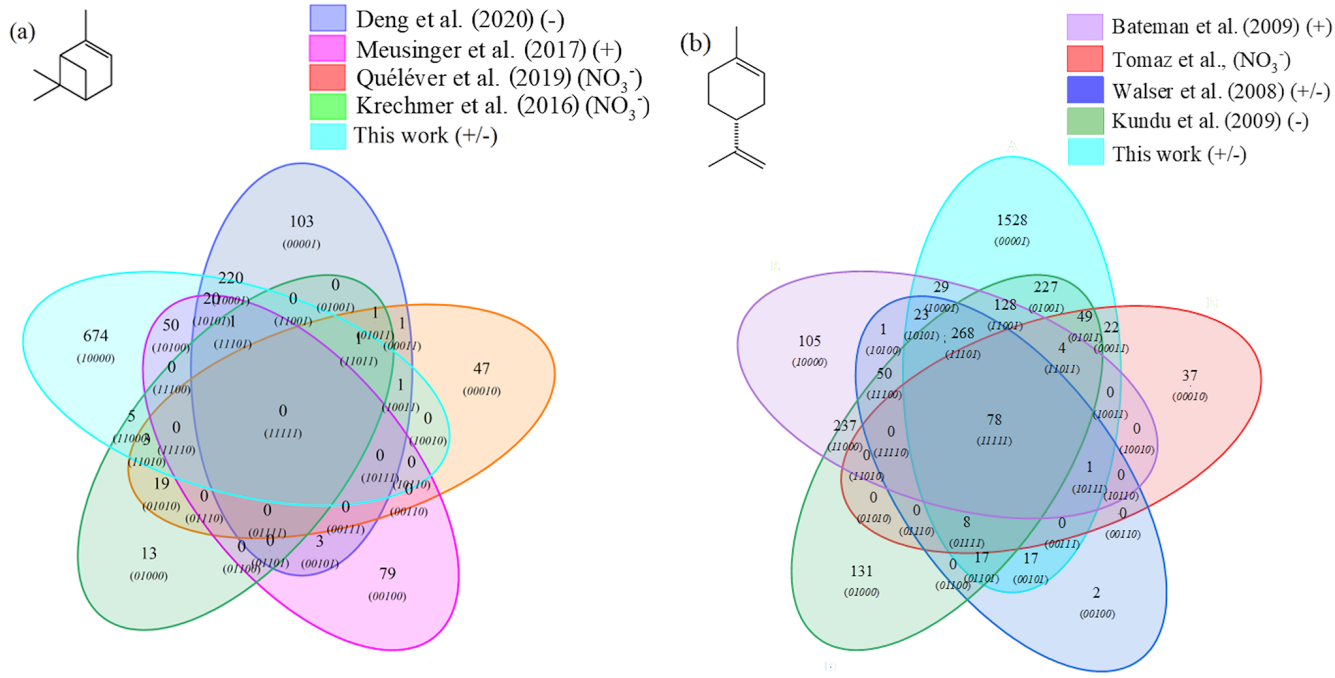

Figure 5. Venn diagrams comparing the oxidation results from ozonolysis and combustion of **(a)** α-pinene and **(b)** limonene (see conditions in Table 1).

For limonene, the similarities with combustion are more important and less spread out. They represent for the different studies 65 % (Kundu et al., 2012), 88 % (Walser et al., 2008), 81 % (Tomaz et al., 2021), and 57 % (Bateman et al., 2009). Moreover, there is a common dataset of 78 chemical formulas which can derive from autoxidation mechanisms. Considering the very different experimental conditions, we must wonder about the impact of the double bonds in this similarity. In the case of limonene, we think their presence will indeed promote the formation of allylic radicals and then peroxide radicals (one of the motors of autoxidation). It is necessary to specify again that different reaction mechanisms can cause the observed similarities. However, the preponderance of autoxidation in so-called cool-flame combustion is obvious, and in atmospheric chemistry, this reaction mechanism is competitive or dominates (Crounse et al., 2013; Jokinen et al., 2014a). If we search for an autoxidation link between these 78 chemical formulas, we observe that 45 % of these chemical formulas meet this condition: a difference of two oxygen atoms between formulas at a constant number of carbon and hydrogen atoms (Table S5 in the Supplement). More precisely, these molecules are centered in a van Krevelen diagram on the ratios $O/C = 0.6$ and $H/C = 1.6$, in the range $0.29 < O/C < 0.77$ and $1.33 < H/C < 1.8$. All oxidized molecules associated with this dataset are presented in Fig. 6. The dispersion of chemical formulas, far from being random, could be correlated with an autoxidation mechanism where the number of carbon and hydrogen atoms is constant.

A 3D representation of all limonene oxidation data is given in the Supplement (Fig. S4a), where DBE is used as the third dimension. From that figure, one can note that products with higher DBE (DBE > 10) are preferably formed under JSR conditions, i.e., at elevated temperature. A 2D representation (OSc versus DBE; Fig. S4b) completes this 3D view. The corresponding chemical formulas with DBE > 10 could correspond to carbonyls and/or cyclic ethers (•QOOH → carbonyl + alkene + OH and/or cyclic ether + OH•). Specificities and similarities of these two oxidation modes (ozonolysis/combustion) were further investigated by plotting the distribution of the number of oxygen atoms in detected chemical formulas (Fig. 7). Indeed, the distribution of the number of oxygen atoms allows, in addition to the van Krevelen diagram, some additional details on these two modes of oxidation to be provided. In ozonolysis, we observed the chemical formulas with the largest number of oxygen atoms. There, oxidation proceeds over a long reaction time where the phenomenon of aging appears through accretion or oligomerization. In combustion, the number of oxygen atoms remains limited to 18, with a lower number of detected chemical formulas compared to the case of ozonolysis. JSR-FIA–HRMS (jet-stirred-reactor flow injection analysis coupled with high-resolution mass spectrometry) data indicated many more sets of chemical formulas differing by two O atoms in the range $C_{10}H_xO_{2-10}$ ($C_{10}H_{12}O_{2-10}$, $C_{10}H_{12}O_{3-9}$, $C_{10}H_{14}O_{2-10}$, $C_{10}H_{14}O_{3-9}$, $C_{10}H_{16}O_{2-8}$, $C_{10}H_{16}O_{3-9}$); see database in Table S4 in the Supplement. Although at this

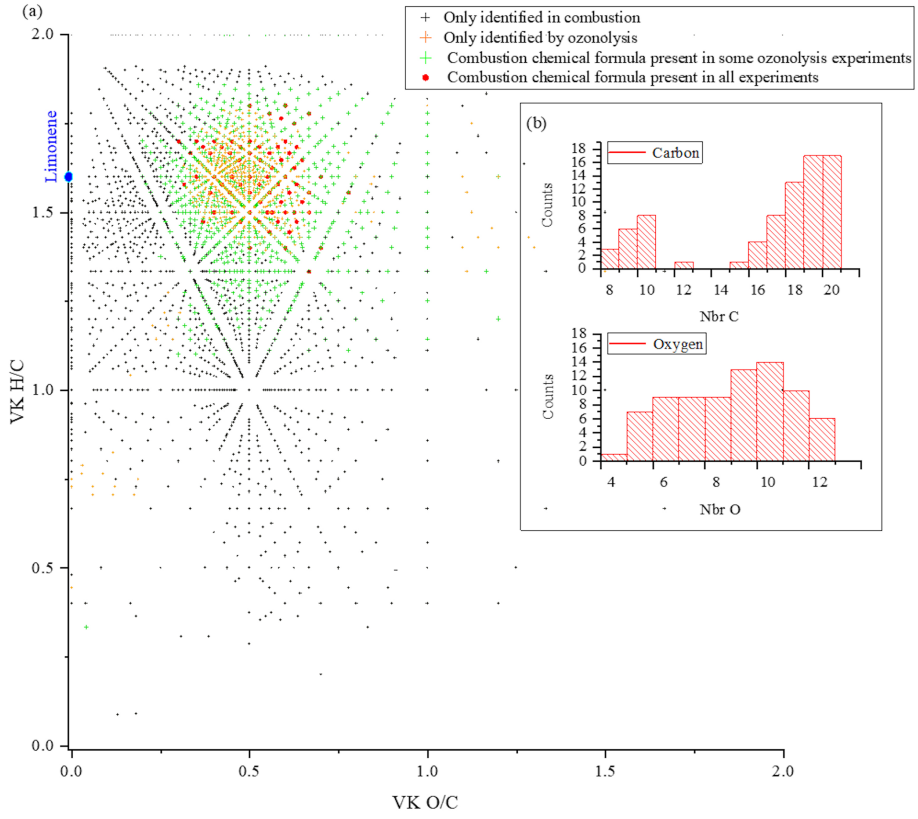

Figure 6. **(a)** Van Krevelen diagram showing specific and common chemical formulas detected after oxidation of limonene by ozonolysis and combustion. **(b)** Distributions of the number of carbon and oxygen atoms in the 78 chemical formulas common to all experiments.

stage one cannot prove these species were formed through autoxidation, their formulas are consistent with autoxidation products. It is in combustion that we observed the highest O/C ratios, indicating the formation of the most oxidized products. This difference, however, does not affect the similarities between the chemical formulas detected in the two modes of oxidation. Finally, the analysis of the parities in oxygen atoms, very similar for the three datasets, confirms that the reaction mechanisms presented in Fig. 3 do not allow a simple link to be established between the oxygen parity of radicals and that of the detected molecular products. The list of these 78 chemical formulas is given in the Supplement.

4.3.2 Identification of common isomers

We identified a set of chemical formulas common to both atmospheric and combustion oxidation modes and suggested that this might result from an autoxidation mechanism. We detected several chemical formulas within this dataset that differ by two oxygen atoms on the same skeleton ($C_{10}H_{16}O_x$). Some of these chemical formulas were previously identified in Fig. 2b or in the 78 common chemical formulas. Focusing on the early stages of limonene oxidation, there are several chemical formulas, starting from $C_{10}H_{16}O_2$ and $C_{10}H_{16}O_3$, which contain an increasing (by two) number

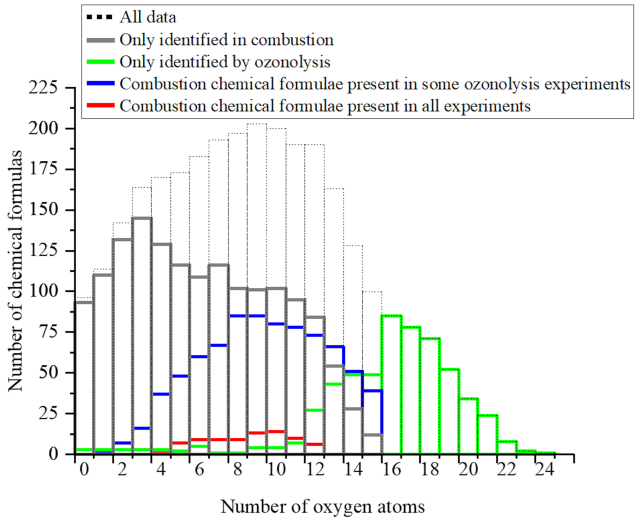

Figure 7. Oxygen number distribution for all the molecules identified for the oxidation of limonene: only in combustion, only in ozonolysis, and common to both processes.

Table 4. Products of multiple addition of oxygen to limonene oxidation product by OH. Chemical formulas are highlighted in red in the Supplement database.

First stages of oxidation	First addition	Second addition	Third addition	Fourth addition	Fifth addition
$C_{10}H_{16}O_2$ (10101) $3.64425 \times 10^{+6}$	$C_{10}H_{16}O_4$ (11101) $1.01228 \times 10^{+7}$	$C_{10}H_{16}O_6$ (11111) $1.99061 \times 10^{+6}$	$C_{10}H_{16}O_8$ (01011) $8.62699 \times 10^{+4}$	$C_{10}H_{16}O_{10}$ (00011) $4.33184 \times 10^{+4}$	$C_{10}H_{16}O_{12}$ (00010)
$C_{10}H_{16}O_3$ (11101) $1.2035E \times 10^{+7}$	$C_{10}H_{16}O_5$ (11111) $5.91408 \times 10^{+6}$	$C_{10}H_{16}O_7$ (11111) $4.90565 \times 10^{+5}$	$C_{10}H_{16}O_9$ (01011) $2.08502 \times 10^{+4}$	$C_{10}H_{16}O_{11}$ (00010)	

Table 5. Isomers of α-pinene and limonene oxidation reported in the literature.

	$C_{10}H_{16}O_2$		$C_{10}H_{16}O_3$	
α-Pinene	Pinonaldehyde	Fang et al. (2017)	Pinonic acid	Fang et al. (2017), Ng et al. (2011), Meusinger et al. (2017)
	Hydroxyketone	Fang et al. (2017)	Hydroxy pinonaldehydes	Fang et al. (2017), Meusinger et al. (2017)
Limonene	Limononaldehyde	Fang et al. (2017), Walser et al. (2008), Bateman et al. (2009)	Limononic acid	Fang et al. (2017), Witkowski and Gierczak (2017), Hammes et al. (2019), Walser et al. (2008), Bateman et al. (2009), Warscheid and Hoffmann (2001)
	4-isopropenyl-methylhydroxy-2-oxocyclohexane	Fang et al. (2017)	7-hydroxy-limononaldehyde	Fang et al. (2017), Walser et al. (2008), Bateman et al. (2009), Meusinger et al. (2017)

of oxygen atoms. Table 4 presents the identified chemical formulas with the Venn index given in parentheses and ion intensity. The index for combustion is the rightmost (xxxx1).

A proposed formation route of the $C_{10}H_{16}O_x$ species is provided in the Supplement (Scheme S5). As can be seen from there, an autoxidation mechanism can start from $\bullet C_{10}H_{15}O_4$ and $\bullet C_{10}H_{15}O_6$, yielding odd-oxygen compounds shown in Table 4. For even-oxygen compounds, one could propose that they are formed after production of RO•, through Reaction (R3) (Fig. S3), or after decomposition of ROOH to yield RO• and OH• and also through oxidation of $\bullet C_{10}H_{17}O_5$ (Fig. S5). Products of the addition of two oxygens are also observed for other chemical formulas within this common dataset. To further investigate the possible formation of common products through atmospheric and combustion chemistries, UHPLC–HRMS experiments were performed. The chemical compounds $C_{10}H_{16}O_2$ for limonene and $C_{10}H_{16}O_3$ for α-pinene were selected considering the availability of standards from suppliers and were among the most frequently reported products in atmospheric-chemistry studies (Table 5). Our study shows the same retention times for these standards and isomers detected in combustion samples (Fig. S6). This result is more obvious for limononaldehyde (11.5 min) than for pinonic acid (3.9 min). In addition, we detected the presence of −OH or −OOH groups by H–D exchange with D_2O and C = O groups through derivatization of carbonyls with 2,4-DNPH for these two chemical formulas (Fig. S7). The low intensity of H–D exchange for α-pinene oxidation products indicates that the pinonic acid isomer is probably present at a low concentration in the sample. Unfortunately, coelution did not fully allow exploitation of MS/MS fragmentation carried out on the two chemical formulas and the formal identification of the two compounds. There is still a lot of characterization work to be done, but the hypothesis of common isomeric products formed through an autoxidation mechanism operating under atmospheric and low-temperature-combustion conditions seems to be confirmed.

5 Conclusion

The oxidation of limonene–oxygen–nitrogen and α-pinene–oxygen–nitrogen mixtures was carried out using a jet-stirred reactor at elevated temperature (590 K), a residence time of 2 s, and atmospheric pressure. The products were analyzed by liquid chromatography, flow injection, and soft-ionization–high-resolution mass spectrometry. H–D exchange and 2,4-dinitrophenyl hydrazine derivatization were used to assess the presence of OOH and C = O groups in products, respectively. We probed the effects of the type of ionization used in mass spectrometry analyses on the de-

tection of oxidation products. Heated electrospray ionization (HESI ±) and atmospheric-pressure chemical ionization (APCI ±) were used. A large dataset was obtained and compared with literature data obtained during the oxidation of limonene and α-pinene under simulated tropospheric and low-temperature-oxidation conditions. This work showed a surprisingly similar set of chemical formulas of products, including oligomers, formed under the two rather different conditions, i.e., cool flames and simulated atmospheric oxidation. Data analysis involving van Krevelen diagrams, oxygen number distribution, oxidation state of carbon, and chemical relationship between molecules indicated that a subset of chemical formulas is common to all experiments independently of experimental conditions. More than 35 % of the chemical formulas detected in combustion chemistry experiments using a JSR have been detected in the studies carried out under atmospheric conditions. Finally, we have outlined the existence of a substantial common dataset of autoxidation products. This result tends to show that autoxidation indeed induces similarity between atmospheric and combustion products. Detailed analysis of our data was performed by UHPLC–MS/MS of selected chemical formulas observed in the literature. Nevertheless, final identification was not possible due to coelutions.

The present JSR data could be useful to atmospheric chemists working in the field of wildfire- and/or biomass-burning-induced air pollution. Considering that low-temperature-oxidation (cool flame) products, i.e., volatile organic compounds, can be emitted from biomass burning, wildfires, and engine exhaust, the present data should be of interest for atmospheric chemists because they complement those obtained in the atmospheric-chemistry literature. It would be interesting to complement the atmospherically relevant data with MS/MS analyses of products and assessment of the presence of hydroperoxyl and carbonyl groups' HOMs. Further MS/MS characterizations are also needed for the products observed in the present work. Finally, a study of the temperature dependence of product formation would be very useful, under both cool-flame conditions and simulated-atmospheric-oxidation conditions.

Data availability. All data sources used in this work are cited in Table 3.

Supplement. The supplement related to this article is available online at: https://doi.org/10.5194/acp-23-5715-2023-supplement.

Author contributions. RB and PD conceived the study. NB, ZD, and ML performed the analysis under the guidance of RB and PD. RB and PD wrote the manuscript. All authors commented on and discussed the manuscript.

Competing interests. The contact author has declared that none of the authors has any competing interests.

Disclaimer. Publisher's note: Copernicus Publications remains neutral with regard to jurisdictional claims in published maps and institutional affiliations.

Acknowledgements. The authors gratefully acknowledge funding from the Labex Caprysses, the Labex Voltaire, CPER, and EFRD (PROMESTOCK and APPROPOR-e projects) as well as the French MESRI for a PhD grant. We also thank the authors of Tomaz et al. (2021) for sharing experimental data on limonene oxidation.

Financial support. This research has been supported by the Labex Caprysses (grant no. ANR-11-LABX-0006-01) and Labex Voltaire (grant no. ANR-10-LABX-100-01).

Review statement. This paper was edited by Andreas Hofzumahaus and reviewed by three anonymous referees.

References

Bailey, H. C. and Norrish, R. G. W.: The oxidation of hexane in the cool-flame region, P. Roy. Soc. Lond. A, 212, 311–330, https://doi.org/10.1098/rspa.1952.0084, 1952.

Bateman, A. P., Nizkorodov, S. A., Laskin, J., and Laskin, A.: Time-resolved molecular characterization of limonene/ozone aerosol using high-resolution electrospray ionization mass spectrometry, Phys. Chem. Chem. Phys., 11, 7931–7942, https://doi.org/10.1039/B905288G, 2009.

Belhadj, N., Benoit, R., Dagaut, P., Lailliau, M., Serinyel, Z., Dayma, G., Khaled, F., Moreau, B., and Foucher, F.: Oxidation of di-n-butyl ether: Experimental characterization of low-temperature products in JSR and RCM, Combust. Flame, 222, 133–144, https://doi.org/10.1016/j.combustflame.2020.08.037, 2020.

Belhadj, N., Benoit, R., Dagaut, P., and Lailliau, M.: Experimental characterization of n-heptane low-temperature oxidation products including keto-hydroperoxides and highly oxygenated organic molecules (HOMs), Combust. Flame, 224, 83–93, https://doi.org/10.1016/j.combustflame.2020.10.021, 2021a.

Belhadj, N., Lailliau, M., Benoit, R., and Dagaut, P.: Towards a Comprehensive Characterization of the Low-Temperature Autoxidation of Di-n-Butyl Ether, Molecules, 26, 7174, https://doi.org/10.3390/molecules26237174, 2021b.

Belhadj, N., Lailliau, M., Benoit, R., and Dagaut, P.: Experimental and kinetic modeling study of n-hexane oxidation. Detection of complex low-temperature products using high-resolution mass spectrometry, Combust. Flame, 233, 111581, https://doi.org/10.1016/j.combustflame.2021.111581, 2021c.

Benoit, R., Belhadj, N., Lailliau, M., and Dagaut, P.: On the similarities and differences between the products of oxidation of hydrocarbons under simulated atmospheric condi-

tions and cool flames, Atmos. Chem. Phys., 21, 7845–7862, https://doi.org/10.5194/acp-21-7845-2021, 2021.

Benson, S. W.: The kinetics and thermochemistry of chemical oxidation with application to combustion and flames, Prog. Energ. Combust. Sci., 7, 125–134, https://doi.org/10.1016/0360-1285(81)90007-1, 1981.

Bernath, P., Boone, C., and Crouse, J.: Wildfire smoke destroys stratospheric ozone, Science, 375, 1292–1295, https://doi.org/10.1126/science.abm5611, 2022.

Berndt, T., Richters, S., Kaethner, R., Voigtländer, J., Stratmann, F., Sipilä, M., Kulmala, M., and Herrmann, H.: Gas-Phase Ozonolysis of Cycloalkenes: Formation of Highly Oxidized RO_2 Radicals and Their Reactions with NO, NO_2, SO_2, and Other RO_2 Radicals, J. Phys. Chem. A, 119, 10336–10348, https://doi.org/10.1021/acs.jpca.5b07295, 2015.

Berndt, T., Richters, S., Jokinen, T., Hyttinen, N., Kurtén, T., Otkjær, R. V., Kjaergaard, H. G., Stratmann, F., Herrmann, H., Sipilä, M., Kulmala, M., and Ehn, M.: Hydroxyl radical-induced formation of highly oxidized organic compounds, Nat. Commun., 7, 13677, https://doi.org/10.1038/ncomms13677, 2016.

Bianchi, F., Kurtén, T., Riva, M., Mohr, C., Rissanen, M. P., Roldin, P., Berndt, T., Crounse, J. D., Wennberg, P. O., Mentel, T. F., Wildt, J., Junninen, H., Jokinen, T., Kulmala, M., Worsnop, D. R., Thornton, J. A., Donahue, N., Kjaergaard, H. G., and Ehn, M.: Highly Oxygenated Organic Molecules (HOM) from Gas-Phase Autoxidation Involving Peroxy Radicals: A Key Contributor to Atmospheric Aerosol, Chem. Rev., 119, 3472–3509, https://doi.org/10.1021/acs.chemrev.8b00395, 2019.

Burke, M., Driscoll, A., Heft-Neal, S., Xue, J., Burney, J., and Wara, M.: The changing risk and burden of wildfire in the United States, P. Natl. Acad. Sci. USA, 118, e2011048118, https://doi.org/10.1073/pnas.2011048118, 2021.

Camredon, M., Hamilton, J. F., Alam, M. S., Wyche, K. P., Carr, T., White, I. R., Monks, P. S., Rickard, A. R., and Bloss, W. J.: Distribution of gaseous and particulate organic composition during dark α-pinene ozonolysis, Atmos. Chem. Phys., 10, 2893–2917, https://doi.org/10.5194/acp-10-2893-2010, 2010.

Cox, R. A. and Cole, J. A.: Chemical aspects of the autoignition of hydrocarbon-air mixtures, Combust. Flame, 60, 109–123, https://doi.org/10.1016/0010-2180(85)90001-X, 1985.

Crounse, J. D., Nielsen, L. B., Jørgensen, S., Kjaergaard, H. G., and Wennberg, P. O.: Autoxidation of organic compounds in the atmosphere, J. Phys. Chem. Lett., 4, 3513, https://doi.org/10.1021/jz4019207, 2013.

Dagaut, P., Cathonnet, M., Rouan, J. P., Foulatier, R., Quilgars, A., Boettner, J. C., Gaillard, F., and James, H.: A jet-stirred reactor for kinetic studies of homogeneous gas-phase reactions at pressures up to ten atmospheres ($\approx$ 1 MPa), J. Phys. E, 19, 207–209, https://doi.org/10.1088/0022-3735/19/3/009, 1986.

Dagaut, P., Cathonnet, M., Boetiner, J. C., and Gaillard, F.: Kinetic Modeling of Propane Oxidation, Combust. Sci. Technol., 56, 23–63, https://doi.org/10.1080/00102208708947080, 1987.

Dagaut, P., Cathonnet, M., Boettner, J. C., and Gaillard, F.: Kinetic modeling of ethylene oxidation, Combust. Flame, 71, 295–312, https://doi.org/10.1016/0010-2180(88)90065-X, 1988.

Deng, Y., Inomata, S., Sato, K., Ramasamy, S., Morino, Y., Enami, S., and Tanimoto, H.: Temperature and acidity dependence of secondary organic aerosol formation from α-pinene ozonolysis with a compact chamber system, Atmos. Chem. Phys., 21, 5983–6003, https://doi.org/10.5194/acp-21-5983-2021, 2021.

Ehn, M., Thornton, J. A., Kleist, E., Sipila, M., Junninen, H., Pullinen, I., Springer, M., Rubach, F., Tillmann, R., Lee, B., Lopez-Hilfiker, F., Andres, S., Acir, I. H., Rissanen, M., Jokinen, T., Schobesberger, S., Kangasluoma, J., Kontkanen, J., Nieminen, T., Kurten, T., Nielsen, L. B., Jorgensen, S., Kjaergaard, H. G., Canagaratna, M., Maso, M. D., Berndt, T., Petaja, T., Wahner, A., Kerminen, V. M., Kulmala, M., Worsnop, D. R., Wildt, J., and Mentel, T. F.: A large source of low-volatility secondary organic aerosol, Nature, 506, 476–479, https://doi.org/10.1038/nature13032, 2014.

Fang, W., Gong, L., and Sheng, L.: Online analysis of secondary organic aerosols from OH-initiated photooxidation and ozonolysis of α-pinene, β-pinene, Δ^3-carene and d-limonene by thermal desorption–photoionisation aerosol mass spectrometry, Environ. Chem., 14, 75–90, https://doi.org/10.1071/EN16128, 2017.

Gilman, J. B., Lerner, B. M., Kuster, W. C., Goldan, P. D., Warneke, C., Veres, P. R., Roberts, J. M., de Gouw, J. A., Burling, I. R., and Yokelson, R. J.: Biomass burning emissions and potential air quality impacts of volatile organic compounds and other trace gases from fuels common in the US, Atmos. Chem. Phys., 15, 13915–13938, https://doi.org/10.5194/acp-15-13915-2015, 2015.

Hammes, J., Lutz, A., Mentel, T., Faxon, C., and Hallquist, M.: Carboxylic acids from limonene oxidation by ozone and hydroxyl radicals: insights into mechanisms derived using a FIGAERO-CIMS, Atmos. Chem. Phys., 19, 13037–13052, https://doi.org/10.5194/acp-19-13037-2019, 2019.

Harvey, B. G., Wright, M. E., and Quintana, R. L.: High-Density Renewable Fuels Based on the Selective Dimerization of Pinenes, Energy Fuels, 24, 267–273, https://doi.org/10.1021/ef900799c, 2010.

Harvey, B. G., Merriman, W. W., and Koontz, T. A.: High-Density Renewable Diesel and Jet Fuels Prepared from Multicyclic Sesquiterpanes and a 1-Hexene-Derived Synthetic Paraffinic Kerosene, Energy Fuels, 29, 2431–2436, https://doi.org/10.1021/ef5027746, 2015.

Hatch, L. E., Jen, C. N., Kreisberg, N. M., Selimovic, V., Yokelson, R. J., Stamatis, C., York, R. A., Foster, D., Stephens, S. L., Goldstein, A. H., and Barsanti, K. C.: Highly Speciated Measurements of Terpenoids Emitted from Laboratory and Mixed-Conifer Forest Prescribed Fires, Environ. Sci. Technol., 53, 9418–9428, https://doi.org/10.1021/acs.est.9b02612, 2019.

Hecht, E. S., Scigelova, M., Eliuk, S., and Makarov, A.: Fundamentals and Advances of Orbitrap Mass Spectrometry, Encyclopedia of Analytical Chemistry, 1–40, https://doi.org/10.1002/9780470027318.a9309.pub2, 2019.

Hu, Y., Fernandez-Anez, N., Smith, T. E. L., and Rein, G.: Review of emissions from smouldering peat fires and their contribution to regional haze episodes, Int. J. Wildland Fire, 27, 293–312, https://doi.org/10.1071/WF17084, 2018.

Huang, W., Saathoff, H., Pajunoja, A., Shen, X., Naumann, K. H., Wagner, R., Virtanen, A., Leisner, T., and Mohr, C.: α-Pinene secondary organic aerosol at low temperature: chemical composition and implications for particle viscosity, Atmos. Chem. Phys., 18, 2883–2898, https://doi.org/10.5194/acp-18-2883-2018, 2018.

Iyer, S., Rissanen, M. P., Valiev, R., Barua, S., Krechmer, J. E., Thornton, J., Ehn, M., and Kurtén, T.: Molecular mechanism for rapid autoxidation in α-pinene ozonolysis, Nat. Commun., 12, 878, https://doi.org/10.1038/s41467-021-21172-w, 2021.

Jokinen, T., Sipilä, M., Richters, S., Kerminen, V.-M., Paasonen, P., Stratmann, F., Worsnop, D., Kulmala, M., Ehn, M., Herrmann, H., and Berndt, T.: Rapid Autoxidation Forms Highly Oxidized RO_2 Radicals in the Atmosphere, Angew. Chem. Int. Edn., 53, 14596–14600, https://doi.org/10.1002/anie.201408566, 2014a.

Jokinen, T., Sipila, M., Richters, S., Kerminen, V. M., Paasonen, P., Stratmann, F., Worsnop, D., Kulmala, M., Ehn, M., and Herrmann, H.: Rapid autoxidation forms highly oxidized RO_2 radicals in the atmosphere, Angew. Chem. Int. Edn., 53, 14596, https://doi.org/10.1002/anie.201408566, 2014b.

Jokinen, T., Berndt, T., Makkonen, R., Kerminen, V.-M., Junninen, H., Paasonen, P., Stratmann, F., Herrmann, H., Guenther, A. B., Worsnop, D. R., Kulmala, M., Ehn, M., and Sipilä, M.: Production of extremely low volatile organic compounds from biogenic emissions: Measured yields and atmospheric implications, P. Natl. Acad. Sci. USA, 112, 7123–7128, https://doi.org/10.1073/pnas.1423977112, 2015.

Kekäläinen, T., Pakarinen, J. M. H., Wickström, K., Lobodin, V. V., McKenna, A. M., and Jänis, J.: Compositional Analysis of Oil Residues by Ultrahigh-Resolution Fourier Transform Ion Cyclotron Resonance Mass Spectrometry, Energy Fuels, 27, 2002–2009, https://doi.org/10.1021/ef301762v, 2013.

Khaykin, S., Legras, B., Bucci, S., Sellitto, P., Isaksen, L., Tencé, F., Bekki, S., Bourassa, A., Rieger, L., Zawada, D., Jumelet, J., and Godin-Beekmann, S.: The 2019/20 Australian wildfires generated a persistent smoke-charged vortex rising up to 35 km altitude, Commun. Earth Environ., 1, 22, https://doi.org/10.1038/s43247-020-00022-5, 2020.

Kobziar, L. N., Pingree, M. R. A., Larson, H., Dreaden, T. J., Green, S., and Smith, J. A.: Pyroaerobiology: the aerosolization and transport of viable microbial life by wildland fire, Ecosphere, 9, e02507, https://doi.org/10.1002/ecs2.2507, 2018.

Korcek, S., Ingold, K. U., Chenier, J. H. B., and Howard, J. A.: Absolute rate constants for hydrocarbon autoxidation. 21. Activation-energies for propagation and correlation of propagation rate constants with carbon-hydrogen bond strengths, Can.J. Chem., 50, 2285–2297, https://doi.org/10.1139/v72-365, 1972.

Kourtchev, I., Doussin, J.-F., Giorio, C., Mahon, B., Wilson, E. M., Maurin, N., Pangui, E., Venables, D. S., Wenger, J. C., and Kalberer, M.: Molecular composition of fresh and aged secondary organic aerosol from a mixture of biogenic volatile compounds: a high-resolution mass spectrometry study, Atmos. Chem. Phys., 15, 5683–5695, https://doi.org/10.5194/acp-15-5683-2015, 2015.

Krechmer, J. E., Groessl, M., Zhang, X., Junninen, H., Massoli, P., Lambe, A. T., Kimmel, J. R., Cubison, M. J., Graf, S., Lin, Y. H., Budisulistiorini, S. H., Zhang, H., Surratt, J. D., Knochenmuss, R., Jayne, J. T., Worsnop, D. R., Jimenez, J. L., and Canagaratna, M. R.: Ion mobility spectrometry–mass spectrometry (IMS–MS) for on- and offline analysis of atmospheric gas and aerosol species, Atmos. Meas. Tech., 9, 3245–3262, https://doi.org/10.5194/amt-9-3245-2016, 2016.

Kristensen, K., Watne, Å. K., Hammes, J., Lutz, A., Petäjä, T., Hallquist, M., Bilde, M., and Glasius, M.: High-Molecular Weight Dimer Esters Are Major Products in Aerosols from α-Pinene Ozonolysis and the Boreal Forest, Environ. Sci. Technol. Lett., 3, 280–285, https://doi.org/10.1021/acs.estlett.6b00152, 2016.

Kroll, J. H., Donahue, N. M., Jimenez, J. L., Kessler, S. H., Canagaratna, M. R., Wilson, K. R., Altieri, K. E., Mazzoleni, L. R., Wozniak, A. S., Bluhm, H., Mysak, E. R., Smith, J. D., Kolb, C. E., and Worsnop, D. R.: Carbon oxidation state as a metric for describing the chemistry of atmospheric organic aerosol, Nat. Chem., 3, 133–139, https://doi.org/10.1038/nchem.948, 2011.

Kundu, S., Fisseha, R., Putman, A. L., Rahn, T. A., and Mazzoleni, L. R.: High molecular weight SOA formation during limonene ozonolysis: insights from ultrahigh-resolution FT-ICR mass spectrometry characterization, Atmos. Chem. Phys., 12, 5523–5536, https://doi.org/10.5194/acp-12-5523-2012, 2012.

Kurtén, T., Rissanen, M. P., Mackeprang, K., Thornton, J. A., Hyttinen, N., Jørgensen, S., Ehn, M., and Kjaergaard, H. G.: Computational Study of Hydrogen Shifts and Ring-Opening Mechanisms in α-Pinene Ozonolysis Products, J. Phys. Chem. A, 119, 11366-11375, https://doi.org/10.1021/acs.jpca.5b08948, 2015.

Melendez-Perez, J. J., Martínez-Mejia, M. J., and Eberlin, M. N.: A reformulated aromaticity index equation under consideration for non-aromatic and non-condensed aromatic cyclic carbonyl compounds, Org. Geochem., 95, 29–33, https://doi.org/10.1016/j.orggeochem.2016.02.002, 2016.

Meusinger, C., Dusek, U., King, S. M., Holzinger, R., Rosenørn, T., Sperlich, P., Julien, M., Remaud, G. S., Bilde, M., Röckmann, T., and Johnson, M. S.: Chemical and isotopic composition of secondary organic aerosol generated by α-pinene ozonolysis, Atmos. Chem. Phys., 17, 6373–6391, https://doi.org/10.5194/acp-17-6373-2017, 2017.

Mewalal, R., Rai, D. K., Kainer, D., Chen, F., Külheim, C., Peter, G. F., and Tuskan, G. A.: Plant-Derived Terpenes: A Feedstock for Specialty Biofuels, Trends Biotechnol., 35, 227–240, https://doi.org/10.1016/j.tibtech.2016.08.003, 2017.

Ng, N. L., Canagaratna, M. R., Jimenez, J. L., Chhabra, P. S., Seinfeld, J. H., and Worsnop, D. R.: Changes in organic aerosol composition with aging inferred from aerosol mass spectra, Atmos. Chem. Phys., 11, 6465–6474, https://doi.org/10.5194/acp-11-6465-2011, 2011.

Nørgaard, A. W., Vibenholt, A., Benassi, M., Clausen, P. A., and Wolkoff, P.: Study of Ozone-Initiated Limonene Reaction Products by Low Temperature Plasma Ionization Mass Spectrometry, J. Am. Soc. Mass Spectrom., 24, 1090–1096, https://doi.org/10.1007/s13361-013-0648-3, 2013.

Nozière, B., Kalberer, M., Claeys, M., Allan, J., D'Anna, B., Decesari, S., Finessi, E., Glasius, M., Grgić, I., Hamilton, J. F., Hoffmann, T., Iinuma, Y., Jaoui, M., Kahnt, A., Kampf, C. J., Kourtchev, I., Maenhaut, W., Marsden, N., Saarikoski, S., Schnelle-Kreis, J., Surratt, J. D., Szidat, S., Szmigielski, R., and Wisthaler, A.: The Molecular Identification of Organic Compounds in the Atmosphere: State of the Art and Challenges, Chem. Rev., 115, 3919–3983, https://doi.org/10.1021/cr5003485, 2015.

Otkjær, R. V., Jakobsen, H. H., Tram, C. M., and Kjaergaard, H. G.: Calculated Hydrogen Shift Rate Constants in Substituted Alkyl Peroxy Radicals, J. Phys. Chem. A, 122, 8665–8673, https://doi.org/10.1021/acs.jpca.8b06223, 2018.

Popovicheva, O. B., Engling, G., Ku, I. T., Timofeev, M. A., and Shonija, N. K.: Aerosol Emissions from Long-lasting Smol-

dering of Boreal Peatlands: Chemical Composition, Markers, and Microstructure, Aerosol Air Qual. Res., 19, 484–503, https://doi.org/10.4209/aaqr.2018.08.0302, 2019.

Prichard, S. J., O'Neill, S. M., Eagle, P., Andreu, A. G., Drye, B., Dubowy, J., Urbanski, S., and Strand, T. M.: Wildland fire emission factors in North America: synthesis of existing data, measurement needs and management applications, Int. J. Wildland Fire, 29, 132–147, https://doi.org/10.1071/WF19066, 2020.

Quéléver, L. L. J., Kristensen, K., Normann Jensen, L., Rosati, B., Teiwes, R., Daellenbach, K. R., Peräkylä, O., Roldin, P., Bossi, R., Pedersen, H. B., Glasius, M., Bilde, M., and Ehn, M.: Effect of temperature on the formation of highly oxygenated organic molecules (HOMs) from alpha-pinene ozonolysis, Atmos. Chem. Phys., 19, 7609–7625, https://doi.org/10.5194/acp-19-7609-2019, 2019.

Riva, M., Rantala, P., Krechmer, J. E., Peräkylä, O., Zhang, Y., Heikkinen, L., Garmash, O., Yan, C., Kulmala, M., Worsnop, D., and Ehn, M.: Evaluating the performance of five different chemical ionization techniques for detecting gaseous oxygenated organic species, Atmos. Meas. Tech., 12, 2403–2421, https://doi.org/10.5194/amt-12-2403-2019, 2019.

Savee, J. D., Papajak, E., Rotavera, B., Huang, H., Eskola, A. J., Welz, O., Sheps, L., Taatjes, C. A., Zádor, J., and Osborn, D. L.: Carbon radicals. Direct observation and kinetics of a hydroperoxyalkyl radical (QOOH), Science, 347, 643–646, https://doi.org/10.1126/science.aaa1495, 2015.

Schneider, E., Czech, H., Popovicheva, O., Lütdke, H., Schnelle-Kreis, J., Khodzher, T., Rüger, C. P., and Zimmermann, R.: Molecular Characterization of Water-Soluble Aerosol Particle Extracts by Ultrahigh-Resolution Mass Spectrometry: Observation of Industrial Emissions and an Atmospherically Aged Wildfire Plume at Lake Baikal, ACS Earth Space Chem., 6, 1095–1107, https://doi.org/10.1021/acsearthspacechem.2c00017, 2022.

Seinfeld, J. H. and Pandis, S. N.: Atmospheric Chemistry and Physics: From Air Pollution to Climate Change, in: 2nd Edn., Wiley-Interscience, Hoboken, NJ, 1232 pp., ISBN 10:0471720186, 2006.

Smith, J. S., Laskin, A., and Laskin, J.: Molecular Characterization of Biomass Burning Aerosols Using High-Resolution Mass Spectrometry, Anal. Chem., 81, 1512–1521, https://doi.org/10.1021/ac8020664, 2009.

Tomaz, S., Wang, D., Zabalegui, N., Li, D., Lamkaddam, H., Bachmeier, F., Vogel, A., Monge, M. E., Perrier, S., Baltensperger, U., George, C., Rissanen, M., Ehn, M., El Haddad, I., and Riva, M.: Structures and reactivity of peroxy radicals and dimeric products revealed by online tandem mass spectrometry, Nat. Commun., 12, 300, https://doi.org/10.1038/s41467-020-20532-2, 2021.

Tröstl, J., Chuang, W. K., Gordon, H., Heinritzi, M., Yan, C., Molteni, U., Ahlm, L., Frege, C., Bianchi, F., Wagner, R., Simon, M., Lehtipalo, K., Williamson, C., Craven, J. S., Duplissy, J., Adamov, A., Almeida, J., Bernhammer, A.-K., Breitenlechner, M., Brilke, S., Dias, A., Ehrhart, S., Flagan, R. C., Franchin, A., Fuchs, C., Guida, R., Gysel, M., Hansel, A., Hoyle, C. R., Jokinen, T., Junninen, H., Kangasluoma, J., Keskinen, H., Kim, J., Krapf, M., Kürten, A., Laaksonen, A., Lawler, M., Leiminger, M., Mathot, S., Möhler, O., Nieminen, T., Onnela, A., Petäjä, T., Piel, F. M., Miettinen, P., Rissanen, M. P., Rondo, L., Sarnela, N., Schobesberger, S., Sengupta, K., Sipilä, M., Smith, J. N., Steiner, G., Tomè, A., Virtanen, A., Wagner, A. C., Weingartner, E., Wimmer, D., Winkler, P. M., Ye, P., Carslaw, K. S., Curtius, J., Dommen, J., Kirkby, J., Kulmala, M., Riipinen, I., Worsnop, D. R., Donahue, N. M., and Baltensperger, U.: The role of low-volatility organic compounds in initial particle growth in the atmosphere, Nature, 533, 527–531, https://doi.org/10.1038/nature18271, 2016.

Van Krevelen, D. W.: Graphical-statistical method for the study of structure and reaction processes of coal, Fuel, 29, 269–284, 1950.

Vereecken, L., Müller, J. F., and Peeters, J.: Low-volatility poly-oxygenates in the OH-initiated atmospheric oxidation of α-pinene: impact of non-traditional peroxyl radical chemistry, Phys. Chem. Chem. Phys., 9, 5241–5248, https://doi.org/10.1039/B708023A, 2007.

Walser, M. L., Desyaterik, Y., Laskin, J., Laskin, A., and Nizkorodov, S. A.: High-resolution mass spectrometric analysis of secondary organic aerosol produced by ozonation of limonene, Phys. Chem. Chem. Phys., 10, 1009–1022, https://doi.org/10.1039/B712620D, 2008.

Wang, Z., Popolan-Vaida, D. M., Chen, B., Moshammer, K., Mohamed, S. Y., Wang, H., Sioud, S., Raji, M. A., Kohse-Höinghaus, K., Hansen, N., Dagaut, P., Leone, S. R., and Sarathy, S. M.: Unraveling the structure and chemical mechanisms of highly oxygenated intermediates in oxidation of organic compounds, P. Natl. Acad. Sci. USA, 114, 13102–13107, https://doi.org/10.1073/pnas.1707564114, 2017.

Wang, Z., Chen, B., Moshammer, K., Popolan-Vaida, D. M., Sioud, S., Shankar, V. S. B., Vuilleumier, D., Tao, T., Ruwe, L., Bräuer, E., Hansen, N., Dagaut, P., Kohse-Höinghaus, K., Raji, M. A., and Sarathy, S. M.: *n*-Heptane cool flame chemistry: Unraveling intermediate species measured in a stirred reactor and motored engine, Combust. Flame, 187, 199–216, https://doi.org/10.1016/j.combustflame.2017.09.003, 2018.

Wang, Z., Ehn, M., Rissanen, M. P., Garmash, O., Quéléver, L., Xing, L., Monge Palacios, M., Rantala, P., Donahue, N. M., Berndt, T., and Sarathy, M.: Efficient alkane oxidation under combustion engine and atmospheric conditions, Commun. Chem., 4, 18, https://doi.org/10.1038/s42004-020-00445-3, 2021.

Warscheid, B. and Hoffmann, T.: Structural elucidation of monoterpene oxidation products by ion trap fragmentation using on-line atmospheric pressure chemical ionisation mass spectrometry in the negative ion mode, Rapid Commun. Mass Spectrom., 15, 2259–2272, https://doi.org/10.1002/rcm.504, 2001.

Witkowski, B. and Gierczak, T.: Characterization of the limonene oxidation products with liquid chromatography coupled to the tandem mass spectrometry, Atmos. Environ., 154, 297–307, https://doi.org/10.1016/j.atmosenv.2017.02.005, 2017.

Wotton, B. M., Gould, J. S., McCaw, W. L., Cheney, N. P., and Taylor, S. W.: Flame temperature and residence time of fires in dry eucalypt forest, Int. J. Wildland Fire, 21, 270–281, https://doi.org/10.1071/WF10127, 2012.

Xie, Q., Su, S., Chen, S., Xu, Y., Cao, D., Chen, J., Ren, L., Yue, S., Zhao, W., Sun, Y., Wang, Z., Tong, H., Su, H., Cheng, Y., Kawamura, K., Jiang, G., Liu, C. Q., and Fu, P.: Molecular characterization of firework-related urban aerosols using Fourier transform ion cyclotron resonance mass spectrometry, Atmos. Chem. Phys., 20, 6803–6820, https://doi.org/10.5194/acp-20-6803-2020, 2020.

Zhang, H., Yee, L. D., Lee, B. H., Curtis, M. P., Worton, D. R., Isaacman-VanWertz, G., Offenberg, J. H., Lewandowski, M., Kleindienst, T. E., Beaver, M. R., Holder, A. L., Lonneman, W. A., Docherty, K. S., Jaoui, M., Pye, H. O. T., Hu, W., Day, D. A., Campuzano-Jost, P., Jimenez, J. L., Guo, H., Weber, R. J., de Gouw, J., Koss, A. R., Edgerton, E. S., Brune, W., Mohr, C., Lopez-Hilfiker, F. D., Lutz, A., Kreisberg, N. M., Spielman, S. R., Hering, S. V., Wilson, K. R., Thornton, J. A., and Goldstein, A. H.: Monoterpenes are the largest source of summertime organic aerosol in the southeastern United States, P. Natl. Acad. Sci. USA, 115, 2038–2043, https://doi.org/10.1073/pnas.1717513115, 2018.

Zhao, Y., Thornton, J. A., and Pye, H. O. T.: Quantitative constraints on autoxidation and dimer formation from direct probing of monoterpene-derived peroxy radical chemistry, P. Natl. Acad. Sci. USA, 115, 12142–12147, https://doi.org/10.1073/pnas.1812147115, 2018.